

BIFURCATIONS AND HYDRA EFFECTS IN ROSENZWEIG-MACARTHUR MODEL

Xiaoqing Lin^{1,2}, Yue Yang³, Yancong Xu^{1,†} and Mu He⁴

Abstract In this paper, a Rosenzweig-MacArthur predator-prey model with intraspecific competition of predators and Holling type II functional response with a prey refuge is investigated by using dynamical approach. We study the number of positive equilibria, the local and global dynamics including Hopf bifurcation, saddle-node bifurcation, Bautin bifurcation. We provide the coexistence of stable and unstable limit cycles. In particular, we show the hydra effect that describes the positive effect of the predator's mortality, as well as the positive effects of prey refuge and intraspecific competition among predators, on the predator's population density. Furthermore, numerical simulations demonstrate the theoretical results including the hydra effect region and trophic cascade.

Keywords Rosenzweig-MacArthur model, intraspecific competition, Bautin bifurcation, hydra effect, prey refuge.

MSC(2010) 34C05, 34C07, 34C23, 34C60.

1. Introduction

Competition, mutualism, and predation are the basic relations of species' trophic interactions in nature. Prey have developed a variety of defense mechanisms, one of which is called refuge where part of the prey population is protected from predation [24]. Many papers have studied the dynamic behavior of the prey-predator model with a prey refuge [5, 12, 15, 23, 24, 29–31]. Wang and his collaborators [24, 30, 31] explored inverted biomass pyramids in the presence of refuge. [32] showed that the increasing number of prey shelters increases the densities of both prey and predators. [16] showed that the existence of shelter can break the limit cycle of a system and solutions reach the desired equilibrium state. [10] proposed two different predator-prey models with Holling type II response function and assumed that the number of prey in the refuge was proportional to the contacts between prey and predators. [1] discussed the hydra effects occurring in Bazykin's predator-prey model without prey refuge, and only located the region for hydra effects with the intrinsic growth rate of prey and the death rate of predators.

[†]The corresponding author: Yancong.xu@cjlu.edu.cn (Y. Xu)

¹Department of Mathematics, China Jiliang University, Hangzhou 310018, China

²Department of Mathematics, Hangzhou Normal University, Hangzhou 311121, China

³Department of Mathematics, Qufu Normal University, Qufu 273165, China

⁴Department of Foundational Mathematics, Xi'an Jiaotong-Liverpool University, Suzhou 215028, China

Email: victorlxq@163.com(X. Lin), yueycn@163.com(Y. Yang),
Yancong.xu@cjlu.edu.cn(Y. Xu), mu.he@xjtlu.edu.cn(M. He)

The following Rosenzweig-MacArthur model with Holling type II functional response has been well investigated in [13] and our model is based on this system:

$$\begin{aligned}\frac{dx}{dt} &= rx\left(1 - \frac{x}{k}\right) - \frac{\beta(1-m)xy}{1+a(1-m)x}, \\ \frac{dy}{dt} &= \frac{c\beta(1-m)xy}{1+a(1-m)x} - \gamma y,\end{aligned}\tag{1.1}$$

where the variables x and y represent (nonnegative) densities of prey and predator, respectively. All parameters $r, \beta, m, a, c, \gamma, s$ are positive numbers for all time $t \geq 0$. Parameter r is the growth rate of prey, k is the carrying capacity of prey, and $r(1 - \frac{x}{k})$ denotes the per capita growth rate of prey in the absence of predator. The parameter γ is the density-independent death/mortality rate of the predator, c is the conversion efficiency (between zero and one due to the second law of thermodynamics). β is the attack rate, and a is the half-saturation constant for what $\frac{\beta x}{1+ax}$ denotes Holling type II functional response. The term mx represents a refuge protection of prey and leaves $(1-m)x$ of prey available to predators, where $m \in [0, 1)$ is the fraction of prey in refuge.

The within species competition for food, shelter, reproduction, or other living resources, is called intraspecific competition [3–22, 25, 27]. Intraspecific competition is a common phenomenon among aquatic and terrestrial species. Two basic types of intraspecific competition have been identified: (1) Interference (adapted) intraspecific competition and (2) exploitation (contest) intraspecific competition. The first type occurs in species that establish hierarchies through aggressive behaviors where one or more individuals within the population hold a dominant status over the others. The second type occurs between individuals of the same population exploiting the same resources and reducing or depleting its availability to others. Many problems with predator-prey models stem from the classic Rosenzweig-MacArthur food chain model, but most existing models ignore the existence of intraspecific competition between predators and don't find the relationship to the hydra effect. To be more realistic, we consider intraspecific competition (also called self-limitation) in our model.

Increased population size caused by increased mortality is now known as a “hydra effect”. This phenomenon describing the seemingly paradoxical increase of a species population size in response to an increase in its mortality rate has been observed in several continuous-time and discrete-time models [17, 18, 26]. From the theoretical point of view, [18] developed a mathematical criterion that guarantees the occurrence of hydra effect in a species embedded in a continuous-time food web model. Their result is quite general because their functions involved can embrace not only a variety of multispecies interactions, but also stage-structured populations. Besides the hydra effect, there is also a positive effect between predator and prey densities when the density is independent of the per capita mortality rate or when the intraspecific competition of the predator increases. Generally speaking, any parameter that affects one species' growth but has no direct impact on the other species in the system, will have a counterintuitive effect on the affected species similar to the hydra effect the increased mortality has. For example, decreasing the conversion efficiency of the predator can increase predator abundance under the same conditions for which hydra effects occur. A predator-prey model with Allee effect and intraspecific competition has been investigated in [19] without analytical analysis, and demonstrated numerically the possibility of multiple hydra effects and

trophic cascade conditional on the existence of bistability on the system, and drawn a conclusion that the Allee effect can bring multiple hydra effects in the predator.

The paper is organized as follows. In section 2, we propose a model that incorporates the intraspecific competition of predators into the Rosenzweig-MacArthur model with the prey refuge. The existence of equilibria and the stability analysis are considered in this section as well. In section 3, we prove the existence of Hopf bifurcation and show the condition that characterizes the stability of the limit cycle from Hopf bifurcation. Furthermore, we show the existence of codimension-two Bautin bifurcation. Numerical simulations are performed in section 4 to verify the theoretical results. The multiple hydra effects and trophic cascade, due to the mortality rate, intraspecific competition and prey refuge, are also found to exhibit the similar dynamics induced by the mortality rate of predator. We conclude and discuss this paper in section 5.

2. Model formulation and equilibria

2.1. Model formulation

Based on the above discussion, in this paper we consider a Rosenzweig-MacArthur model with intraspecific interference of predator and Holling type II functional response with prey refuge as follows:

$$\begin{aligned}\frac{dx}{dt} &= rx\left(1 - \frac{x}{k}\right) - \frac{\beta(1-m)xy}{1+a(1-m)x}, \\ \frac{dy}{dt} &= \frac{c\beta(1-m)xy}{1+a(1-m)x} - \gamma y - sy^2,\end{aligned}\tag{2.1}$$

where $x, y, r, k, \beta, a, m, c, \gamma$ have the same meaning as those in model (1.1). Due to the intraspecific competition for resources, the death caused by this intraspecific interference effect exists in predators, i.e., the per capita mortality rate of intraspecific competition is proportional to the number of predators which is denoted as sy .

Since system (2.1) is a biological system, then it is studied in $\mathbb{R}_+^2 = \{(x, y) | x \geq 0, y \geq 0\}$, and the feasible region of system (2.1) is

$$\Omega = \{(x, y) | 0 \leq x \leq k, 0 \leq y \leq \frac{c\beta(1-m)k}{s(1+a(1-m)k)} - \frac{\gamma}{s}\}.$$

2.2. Equilibria and stability

In this section, we will discuss the existence of equilibria and their stability. System (2.1) always has two boundary equilibria $E_0(0, 0)$ and $E_k(k, 0)$. Through a simple analysis of the eigenvalue of Jacobian matrix of system (2.1), we can easily get conclusion as follows.

Theorem 2.1. *System (2.1) always has two boundary equilibria $E_0(0, 0)$ and $E_k(k, 0)$. $E_0(0, 0)$ is a hyperbolic saddle. $E_k(k, 0)$ is a degenerate equilibrium if $\gamma = \frac{\beta ck(m-1)}{ak(m-1)-1}$, a hyperbolic saddle if $\gamma < \frac{\beta ck(m-1)}{ak(m-1)-1}$, a hyperbolic stable node if $\gamma > \frac{\beta ck(m-1)}{ak(m-1)-1}$, respectively.*

Next, we consider the existence of positive equilibria $E^*(x^*, y^*)$ of system (2.1). For any positive equilibrium $E^*(x^*, y^*)$, its coordinates satisfy

$$y^* = \frac{r(1 - \frac{x^*}{k})(1 + a(1 - m)x^*)}{\beta(1 - m)} \quad \text{or} \quad \frac{(m - 1)x^*(\beta c - a\gamma) + \gamma}{s(a(m - 1)x^* - 1)}, \quad (2.2)$$

and the coordinate x^* should be the positive root of the following cubic equation

$$g(x) = x^3 + b_1x^2 + b_2x + b_3 = 0, \quad (2.3)$$

where

$$\begin{aligned} b_1 &= \frac{ak(1 - m) - 2}{-a(1 - m)}, \\ b_2 &= \frac{\beta k(1 - m)^2(\beta c - a\gamma) + rs(1 - 2ak(1 - m))}{a^2(1 - m)^2rs}, \\ b_3 &= -\frac{k(rs + \beta\gamma(1 - m))}{a^2(1 - m)^2rs}. \end{aligned}$$

Note that the above equation may have one, two, or three positive roots for $x \in (0, k)$. Thus, system (2.1) will have one, two, or three positive equilibria. Moreover, we can easily get that

$$x_1 + x_2 + x_3 = -b_1, \quad x_1x_2 + x_1x_3 + x_2x_3 = b_2, \quad x_1x_2x_3 = -b_3$$

by Vieta theorem and

$$g'(x) = 3x^2 + 2b_1x + b_2. \quad (2.4)$$

By the roots of the cubic algebraic equation, we denote

$$\begin{aligned} \tilde{B} &= b_1^2 - 3b_2, \\ \Delta &= -4\tilde{B}^3 + (3b_1\tilde{B} - b_1^3 + 27b_3)^2. \end{aligned}$$

Since the coefficient of the cubic equation $b_3 < 0$, then system (2.1) has at most three positive equilibria in addition to two boundary equilibria $E_0(0, 0)$ and $E_k(k, 0)$. According to the graph of $g(x)$, we have the following lemma.

Lemma 2.1. *When $b_3 < 0$, system (2.1) may have one, two or three positive equilibria. More precisely,*

- (1) *when $\Delta > 0$, system (2.1) has a unique positive equilibrium $\bar{E}_1^*(\bar{x}_1^*, \bar{y}_1^*)$, which is a hyperbolic stable node or focus for $\text{tr}(J(\bar{E}_1^*)) < 0$, a hyperbolic unstable node or focus for $\text{tr}(J(\bar{E}_1^*)) > 0$, and a weak focus or center for $\text{tr}(J(\bar{E}_1^*)) = 0$;*
- (2) *when $\Delta = 0$ and*
 - (a) *$\tilde{B} > 0$, $b_1 < 0$ and $b_2 > 0$, system (2.1) have two different positive equilibria: a degenerate equilibrium $\tilde{E}^*(\tilde{x}^*, \tilde{y}^*)$ and an elementary equilibrium $\bar{E}_1^*(\bar{x}_1^*, \bar{y}_1^*)$ (or $\bar{E}_3^*(\bar{x}_3^*, \bar{y}_3^*)$). \bar{E}_i^* ($i = 1$ or 3) are hyperbolic stable node or focus for $\text{tr}(J_i) < 0$, a hyperbolic unstable node or focus for $\text{tr}(J_i) > 0$, and a weak focus or center for $\text{tr}(J_i) = 0$, where $\bar{x}_1^* < \tilde{x}^* < \bar{x}_3^*$;*
 - (b) *$\tilde{B} = 0$ and $b_1 < 0$, system (2.1) has a unique positive equilibrium $\hat{E}^*(\hat{x}^*, \hat{y}^*) = (-\frac{b_1}{3}, \frac{r(b_1 + 3k)(3 - ab_1(1 - m))}{9\beta k(1 - m)})$;*

(3) when $\Delta < 0$, $b_1 < 0$ and $b_2 > 0$, system (2.1) has three different positive equilibria: $\bar{E}_i^*(\bar{x}_i^*, \bar{y}_i^*) (i = 1, 2, 3)$. $\bar{E}_2^*(\bar{x}_2^*, \bar{y}_2^*)$ is a hyperbolic saddle. $\bar{E}_i^* (i = 1, 3)$ are hyperbolic stable node or focus for $\text{tr}(J_i) < 0$, a hyperbolic unstable node or focus for $\text{tr}(J_i) > 0$, and a weak focus or center for $\text{tr}(J_i) = 0$, where $0 < \bar{x}_1^* < \bar{x}_2^* < \bar{x}_3^* < k$.

Proof. By using the first equation the the second equation in system (2.1), we can simplify the Jacobian matrix of system (2.1) at $E(x, y)$ with the following form

$$J(E) = \begin{pmatrix} \frac{r(x+a(m-1)(k-2x)x)}{k(-1+a(m-1)x)} & -\frac{\beta(1-m)x}{1+a(1-m)x} \\ \frac{cr(k-x)}{k-ak(m-1)x} & \gamma - \frac{c(m-1)x\beta}{-1+a(m-1)x} \end{pmatrix}, \quad (2.5)$$

and

$$\det(J(E)) = \frac{1}{k(-1+a(m-1)x)^2} x [-c\beta(m-1)r(k+ak(m-1)x-2a(m-1)x^2) + r\gamma(1+a(m-1)(k-2x))(-1+a(m-1)x)].$$

To solve the $g(x) = 0$, we have

$$c = \frac{(-1+a(m-1)x)(rs(k-x)(-1+a(m-1)x) + k\beta\gamma(m-1))}{k(1-m)^2x\beta^2}. \quad (2.6)$$

By substituting (2.6) into above $\det(J(E))$, the determinant of matrix $J(E)$ becomes

$$\begin{aligned} & \det(J(E)) \\ &= \frac{r(x-k)(rs(a(m-1)x-1)(ak(m-1)x-2a(m-1)x^2+k) + \beta\gamma k(m-1))}{\beta k^2(m-1)(a(m-1)x-1)} \\ &= \frac{a^2(m-1)r^2s(k-x)}{\beta k^2(a(m-1)x-1)} (xg'(x) - g(x)) \\ &= \frac{a^2(m-1)r^2sx(k-x)}{\beta k^2(a(m-1)x-1)} g'(x). \end{aligned} \quad (2.7)$$

From (2.7), we know that $\frac{r(x-k)}{k^2(m-1)(-1+a(m-1)x)\beta} > 0$, thus the sign of $\det(J(E))$ is equal to the sign of derivative of $g(x)$. From the equation (2.3) and the property of $g'(x)$, we can complete the proof. \square

3. Bifurcation analysis

In this section, we will give a detailed analysis of Hopf bifurcation and generalized Hopf bifurcation to determine the stability of limit cycle of system (2.1), and obtain the Lyapunov coefficient to indicate the existence of Bautin bifurcation.

3.1. Hopf bifurcation

From the previous section, system (2.1) has one, two, or three equilibrium points under the conditions of Lemma 2.1. Equilibria \bar{E}_1^* and \bar{E}_3^* are always saddles,

so their stability will not change, and it is impossible for the occurrence of Hopf bifurcation. Therefore, we will choose the equilibrium \bar{E}_2^* to analyze the existence of Hopf bifurcation as a pair of pure imaginary eigenvalue exists under the conditions $\det(J) > 0$ and $\text{tr}(J) = 0$.

The Jacobian matrix at $\bar{E}_2^*(x^*, y^*)$ is

$$J(\bar{E}_2^*) = \begin{pmatrix} \frac{r(a(m-1)x^*(k-2x^*)+x^*)}{k(a(m-1)x^*-1)} & -\frac{\beta(m-1)x^*}{a(m-1)x^*-1} \\ \frac{cr(k-x^*)}{k-ak(m-1)x^*} & \gamma - \frac{\beta c(m-1)x^*}{a(m-1)x^*-1} \end{pmatrix}.$$

Let $\gamma = -\frac{x^*(a(m-1)r(k-2x^*)-\beta ck(m-1)+r)}{k(a(m-1)x^*-1)} \equiv \gamma_H$. Now we suppose that the following three conditions are satisfied at $\gamma = \gamma_H$.

(H₁) $\text{tr}(J(\bar{E}_2^*; \gamma = \gamma_H)) = 0$;

(H₂) $\det(J(\bar{E}_2^*; \gamma = \gamma_H)) > 0$;

(H₃) If $\lambda(\gamma)$ is the complex eigenvalue of $J(\bar{E}_2^*)$, then $\frac{d}{d\gamma}(Re(\lambda(\gamma)))|_{\gamma=\gamma_H} \neq 0$.

Then \bar{E}_2^* loses its stability through a Hopf bifurcation at $\gamma = \gamma_H$.

It is easy to obtain that the real part $Re(\lambda(\gamma))$ of a complex eigenvalue is as follows:

$$Re(\lambda(\gamma)) = \frac{\text{tr}(J(\bar{E}_2^*))}{2} = \frac{1}{2} \left(\frac{x^*(a(m-1)r(k-2x^*)-\beta ck(m-1)+r)}{k(a(m-1)x^*-1)} + \gamma \right),$$

which yields that

$$\begin{aligned} & \frac{d}{d\gamma} Re(\lambda(\gamma)) \\ &= \frac{k(k(m-1)(2a(m-1)x^*-1)(ar-\beta c) + r(6a(m-1)x^*(ax^*(1-m)+1)-1))}{2(k(a(m-1)x^*-1))^2} \\ & \times \frac{dx^*}{d\gamma} + \frac{1}{2}. \end{aligned} \tag{3.1}$$

Then we need to determine the sign of (3.1) which is the Hopf bifurcation threshold for the parameterisations considered here.

3.2. Bautin bifurcation (Generalized Hopf bifurcation)

From the previous analysis, we know that there exist one, two or three equilibria, and it is sufficient to analyze the Bautin bifurcation (generalized Hopf bifurcation) at point $\hat{E}^*(\hat{x}^*, \hat{y}^*)$ with $\hat{x}^* = \frac{ak(m-1)+2}{a(1-m)}$, $\hat{y}^* = -\frac{2r(ak(m-1)+1)(ak(m-1)+3)}{a\beta k(1-m)^2}$. Since the equilibrium \hat{E}^* is not at the origin $O(0, 0)$, we need to translate the coordinates of \hat{E}^* to origin by $X = x - \hat{x}^*$, $Y = y - \hat{y}^*$. System (2.1) can be transformed as

$$\begin{cases} \frac{dX}{dt} = r(X + \hat{x}^*) \left(1 - \frac{X + \hat{x}^*}{k} \right) - \frac{\beta(1-m)(X + \hat{x}^*)(Y + \hat{y}^*)}{a(1-m)(X + \hat{x}^*) + 1}, \\ \frac{dY}{dt} = \frac{\beta c(1-m)(X + \hat{x}^*)(Y + \hat{y}^*)}{a(1-m)(X + \hat{x}^*) + 1} - s(Y + \hat{y}^*)^2 - \gamma(Y + \hat{y}^*). \end{cases} \tag{3.2}$$

The Jacobian matrix of system (3.2) at origin $(0, 0)$ is

$$J_0 = \begin{pmatrix} \frac{(ak(m-1)+2)(3ak(m-1)+5)r}{ak(ak(m-1)+3)(m-1)} & -\frac{(ak(m-1)+2)\beta}{a(ak(m-1)+3)} \\ \frac{2c(ak(m-1)+1)r}{ak(ak(m-1)+3)(m-1)} & -\frac{(ak(m-1)+2)(3ak(m-1)+5)r}{ak(ak(m-1)+3)(m-1)} \end{pmatrix}.$$

Then the characteristic equation of J_0 is

$$f(\lambda) \equiv \lambda^2 + \text{tr}(J_0)\lambda + \det(J_0) = 0,$$

where

$$\begin{aligned} & \text{tr}(J_0) \\ = & -\frac{\beta(m-1)r(ak(m-1)+2)(3ak(m-1)+5)+4rs(ak(m-1)+1)(ak(m-1)+3)^2}{a\beta k(1-m)^2(ak(m-1)+3)} \\ & -\frac{\beta k(1-m)^2(\beta c(ak(m-1)+2)+a\gamma(-akm+ak-3))}{a\beta k(1-m)^2(ak(m-1)+3)}, \\ & \det(J_0) \\ = & \frac{r(ak(m-1)+2)(\beta k(1-m)^2(\beta c(3ak(m-1)+4)+a\gamma(-3ak(m-1)-5))}{a^2\beta k^2(m-1)^3(ak(m-1)+3)} \\ & +\frac{4rs(ak(m-1)+1)(ak(m-1)+3)(3ak(m-1)+5)}{a^2\beta k^2(m-1)^3(ak(m-1)+3)}. \end{aligned}$$

Assume

$$a < \frac{rs + kc\beta^2(1-m)^2}{2krs(1-m) + \gamma k\beta(1-m)^2},$$

and the above hypothesis holds. The Jacobian matrix J_0 has a pair of purely imaginary roots $\pm i\omega$ when

$$s = -\frac{a\beta k(1-m)^2 \left(\frac{\beta c(ak(m-1)+2)+a\gamma(-akm+ak-3)}{a(ak(m-1)+3)} + \frac{r(ak(m-1)+2)(3ak(m-1)+5)}{ak(m-1)(ak(m-1)+3)} \right)}{4r(ak(m-1)+1)(ak(m-1)+3)} \quad (3.3)$$

with

$$\omega = \sqrt{-\frac{r(ak(m-1)+2)(r(ak(m-1)+2)(3ak(m-1)+5)^2 - 2\beta ck(m-1)(ak(m-1)+1))}{a^2 k^2 (1-m)^2 (ak(m-1)+3)^2}}. \quad (3.4)$$

By (3.3) and (3.4), we obtain the vectors

$$q = (q_1, q_2)^T,$$

where

$$\begin{aligned} q_1 = & \frac{\sqrt{r(ak(m-1)+2)(r(ak(m-1)+2)(3ak(m-1)+5)^2 - 2\beta ck(m-1)(ak(m-1)+1))}}{2cr(ak(m-1)+1)} \\ & + \frac{r(ak(m-1)+2)(3ak(m-1)+5)}{2cr(ak(m-1)+1)}, \end{aligned}$$

$$q_2 = 1,$$

and

$$p = (p_1, p_2)^T,$$

with

$$p_1 = \frac{i\sqrt{r(-(ak(m-1)+2))(r(ak(m-1)+2)(3ak(m-1)+5)^2-2\beta ck(m-1)(ak(m-1)+1))}}{\beta k(m-1)(ak(m-1)+2)} - \frac{r(ak(m-1)+2)(3ak(m-1)+5)}{\beta k(m-1)(ak(m-1)+2)},$$

$p_2 = 1.$

Vectors p and q satisfy

$$Jq = i\sqrt{ab}q, \quad J^T p = -i\sqrt{ab}p, \quad \langle p, q \rangle = 1.$$

Further calculation leads to

$$B(\xi, \eta) = \begin{pmatrix} 0 \\ -\xi_1\eta_3 - \xi_3\eta_1 \\ \xi_1\eta_2 + \xi_2\eta_1 \end{pmatrix}, \quad C(\xi, \eta, \tau) = \begin{pmatrix} 0 \\ 0 \\ 0 \end{pmatrix}.$$

It is easy to calculate J_0^{-1} and $(2i\omega E - J_0)^{-1}$. We have

$$l_1 = \frac{1}{2\omega} \operatorname{Re} [\langle p, C(q, q, \bar{q}) \rangle - 2 \langle p, B(q, J^{-1}B(q, \bar{q})) \rangle + \langle p, B(\bar{q}, (2i\omega E - J)^{-1}B(q, q)) \rangle] \\ = \frac{\Delta}{6(\alpha + 1)^2 c^2 r^2 \omega ((\alpha + 2)(3\alpha + 5)^2 r - 2(\alpha + 1)\beta ck(m - 1))},$$

where

$$\alpha = ak(m - 1), \\ \Delta = \alpha(\alpha + 3)(3\alpha + 5)((\alpha + 2)k(m - 1)r((\alpha + 1)\beta c(2\alpha(\alpha + 3)\omega + 5) - a(\alpha + 3)(3\alpha + 5)\omega) + a(\alpha + 3)k(m - 1)\omega\sqrt{(\alpha + 2)r(2(\alpha + 1)\beta ck(m - 1) - (\alpha + 2)(3\alpha + 5)^2 r) + (3\alpha + 5)(\alpha + 2)^2 r^2(9\alpha + (\alpha + 1)\beta ck(m - 1) + 15)}). \tag{3.5}$$

Therefore we obtain the following theorem:

Theorem 3.1. *System (2.1) exhibits codimension-2 Bautin bifurcation at the equilibrium $\widehat{E}^*(\widehat{x}^*, \widehat{y}^*)$ if and only if the following condition is satisfied:*

$$s = -\frac{a\beta k(1 - m)^2 \left(\frac{\beta c(ak(m-1)+2)+a\gamma(-akm+ak-3)}{a(ak(m-1)+3)} + \frac{r(ak(m-1)+2)(3ak(m-1)+5)}{ak(m-1)(ak(m-1)+3)} \right)}{4r(ak(m-1)+1)(ak(m-1)+3)}$$

and $\Delta = 0,$

Where Δ is defined by (3.5).

4. Numerical simulations

In this section, we will summarize the results that we have proved in the previous sections for model (2.1). We choose a set of the following parameters:

$$r = 10, \beta = 0.6, m = 0.4, a = 0.1, c = 0.02, \gamma = 0.09, \tag{4.1}$$

which are taken from [13]. In this paper, we take $k = 1002.22$.

Firstly, we consider the role of intraspecific competition of predators by taking the intraspecific competition constant s as the primary bifurcation parameter. Fixing the rest of the parameters as (4.1) and $k = 1002.22$, we obtain one-parameter bifurcation diagrams. As shown in Fig. 1 (a), there are a subcritical Hopf bifurcation point $HB(491.42, 431.59)$ at $s = 6.04 \times 10^{-5}$, and two saddle-node bifurcation points $SN_1(130.16, 212.94)$ as $s = 7.69 \times 10^{-5}$, and $SN_2(445.95, 427.95)$ as $s = 5.99 \times 10^{-5}$. As noted in [18] for stable systems, the predator has a hydra effect if and only if $\det(J)$ and M_{ii} have the same sign, where M_{ii} denotes the i th principle minor of the Jacobian, i.e., the determinant of the matrix which the i th row and i th column of the Jacobian matrix has been removed. It should satisfy the condition $\frac{\partial}{\partial y}(\frac{1}{y} \frac{dy}{dt}) < 0$ for system (2.1), i.e., $\frac{\partial}{\partial y}(\frac{1}{y} \frac{c\beta(1-m)xy}{1+a(1-m)x} - \gamma y - sy^2) = -s < 0$. Then there are two hydra effect intervals $5.99 \times 10^{-5} \leq s \leq 6.04 \times 10^{-5}$ and $5.99 \times 10^{-5} \leq s \leq 7.69 \times 10^{-5}$. Note that, the second region also denotes the region with three positive equilibria, and the transition from instability to stability via the Hopf bifurcation occurs. The region for multiple hydra effects is $5.99 \times 10^{-5} \leq s \leq 6.04 \times 10^{-5}$.

There are three coexisting positive equilibria (two unstable equilibria, one stable equilibrium). When intraspecific interference of predators is stronger and stronger, the predator population will extinct for all nonnegative initial value (Fig. 1 (b)). We continue from the Hopf bifurcation point (HB) and obtain a family of unstable limit cycles with periods approaching $+\infty$, i.e., the limit cycles are actually approaching a homoclinic orbit connecting $E^*(417.13, 399.50)$ (see Fig. 1 (c) (d)) and relaxation oscillations occur [11]. According to Fig. 1 (a) and Fig. 1 (b), the density of prey remains increasing while the density of predator increases in a short parameter region and then decreases sharply when the intensity of intraspecific competition increases up to the threshold value $s = 7.69 \times 10^{-5}$. That is to say, the intraspecific competition within predators do benefit them in some situations. However, it will have a negative effect if the intraspecific competition is too intense beyond the threshold value $s = 7.69 \times 10^{-5}$. There exists a critical interval $s \in [5.99 \times 10^{-5}, 7.69 \times 10^{-5}]$ for the evolution of predators. If $s \geq 6.04 \times 10^{-5}$, so-called tropic cascade takes place, that is, the density of predator decreases while the density of prey increases. Once the intraspecific competition constant s enters the interval, the density of prey will increase rapidly like a S -type. However, the density of predator will increase until it reaches the maximum, then the density of predator will decrease promptly as the intraspecific competition becomes stronger.

Secondly, we take the half-saturation constant a as the primary bifurcation parameter, $s = 0.01$, and keep other parameters fixed as (4.1). There are two Hopf bifurcation points: a supercritical Hopf bifurcation point $HB_1(57.84, 28.82)$ at $a = 0.0029$ and a subcritical Hopf bifurcation point $HB_2(387.74, 64.60)$ at $a = 0.012$, and a saddle-node bifurcation point of limit cycles $SN(77.8, 66.9)$ at $a = 0.012045$ with period $T = 15.081$. (Fig. 2 (a), (b)). There are two coexisting limit cycles: the inner one is unstable, and the outer one is stable when the parameter $a = 0.0120058$. Further, there is only one limit cycle as $a = 0.01201$, shown in Fig. 3 (a) and (b). According to Fig. 2, we know that the small half-saturation constant a enhances the density of predator. However, the increased half-saturation constant a will have a negative effect on the density of predator, while it still has a positive effect on the density of prey. Interestingly, once the parameter a passes the critical value 0.01202, the density of predator will decrease quickly.

Thirdly, we take the prey refuge constant m as the primary bifurcation param-

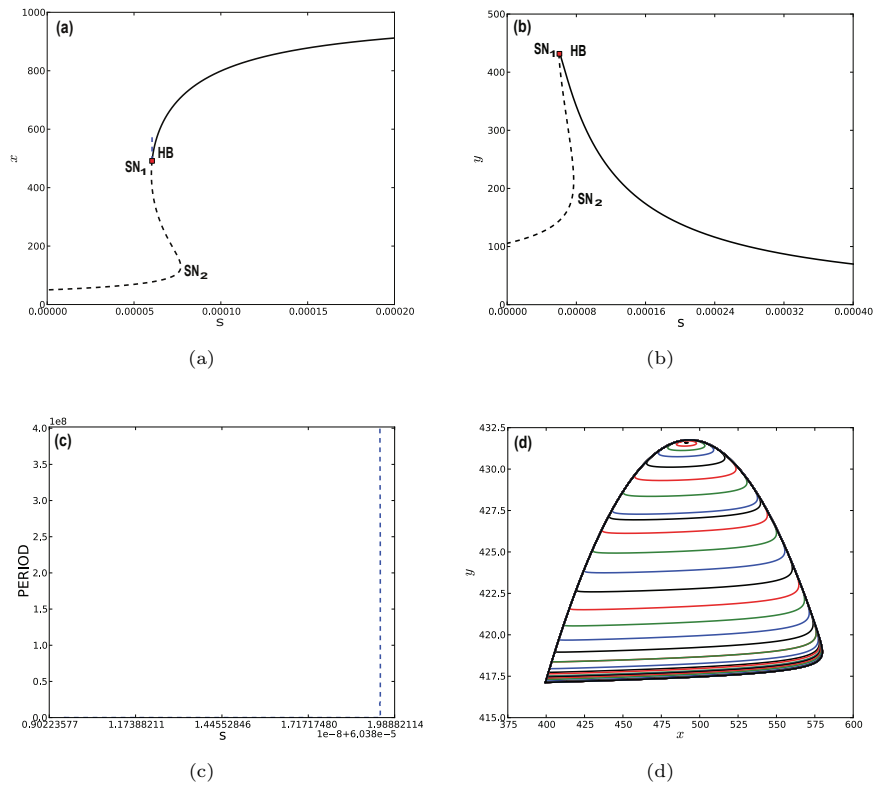


Figure 1. Bifurcation diagram and phase portrait of model (2.1). HB , SN_1 and SN_2 denote the subcritical Hopf bifurcation point, two saddle-node bifurcation points. (a) One-parameter bifurcation diagram for s vs x . (b) One-parameter bifurcation diagram for s vs y . (c) Bifurcation diagram of s vs the period. (d) A family of unstable limit cycles approach a homoclinic orbit in phase portrait. Relaxation oscillations occur.

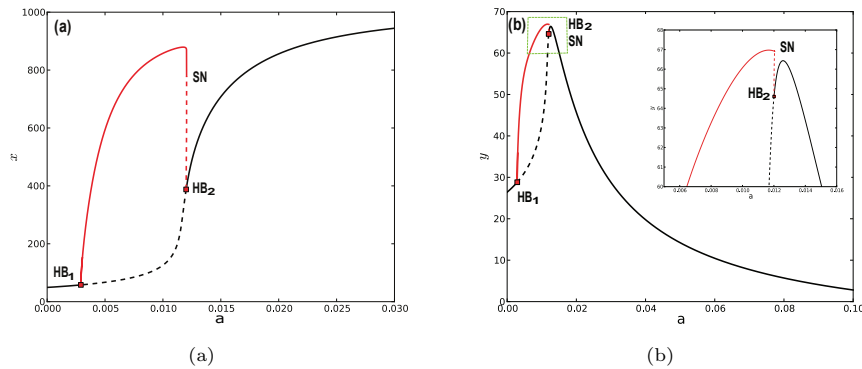


Figure 2. One-parameter bifurcation diagram of model (2.1). (a) One-parameter bifurcation diagram with a vs x . (b) One-parameter bifurcation diagram for a vs y . Here HB_1 , HB_2 and SN denote, the supercritical Hopf bifurcation point, the subcritical Hopf bifurcation point and saddle-node bifurcation point of limit cycles, respectively.

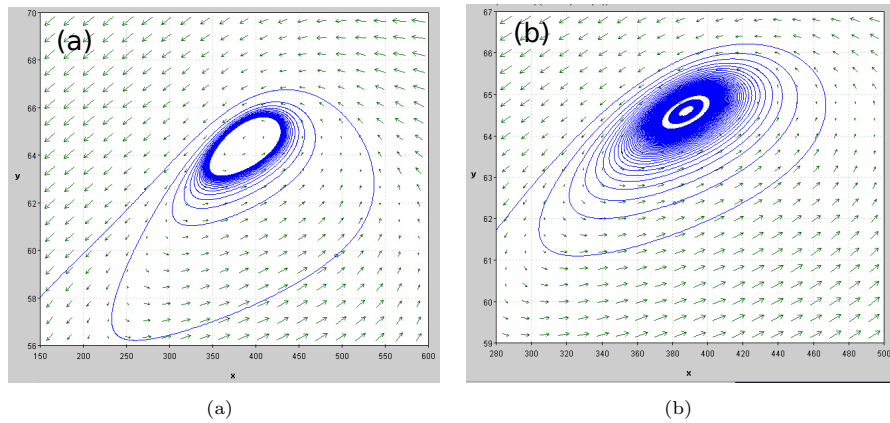


Figure 3. Phase portrait of limit cycles in model (2.1). (a) One limit cycle at $a = 0.01201$. (b) For the parameters $a = 0.0120058$, the positive equilibrium point is an attractor, surrounded by two limit cycles: the inner one is unstable and the outer one is stable.

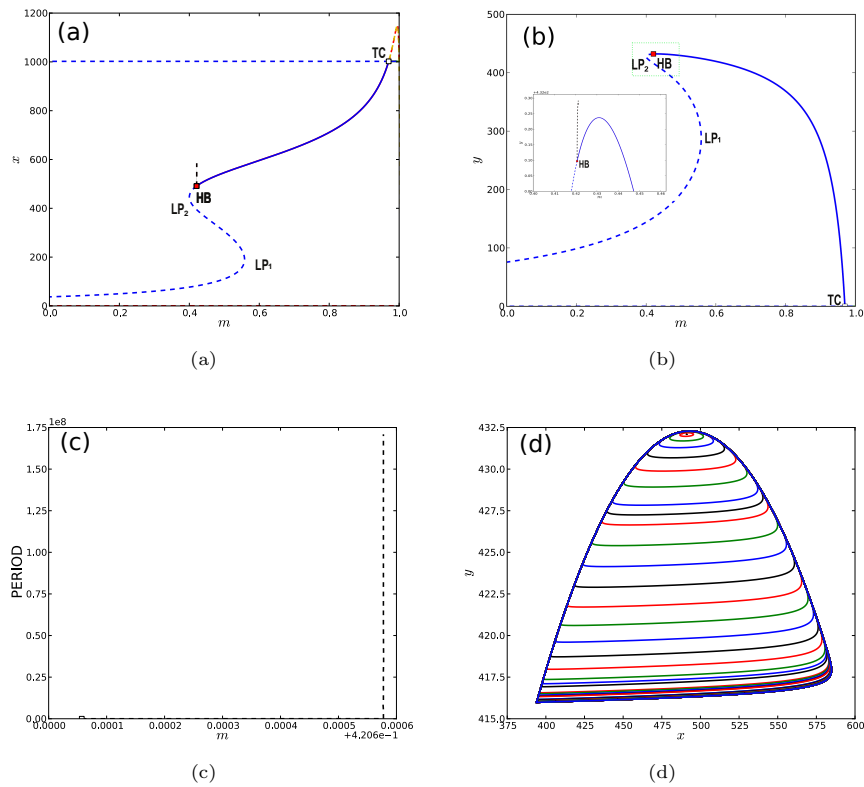


Figure 4. Bifurcation diagrams of model (2.1). *HB*, *TC* and *LP* denote the Hopf bifurcation point, transcritical bifurcation point. (a) One-parameter bifurcation diagram for m vs x . (b) One-parameter bifurcation diagram for m vs y . (c) Bifurcation diagram of m vs the period. (d) A family of unstable limit cycles approach a homoclinic orbit in phase portrait, and relaxation oscillations occur.

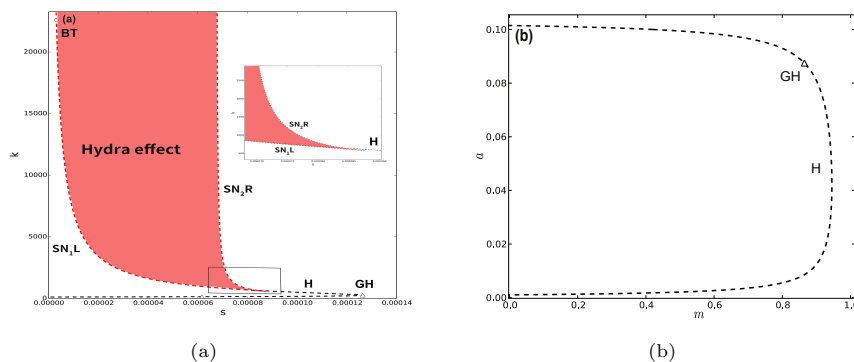


Figure 5. Two-parameter bifurcation diagrams of model (2.1). (a) Bifurcation diagram in s - k parameter space. (b) Hopf bifurcation diagram in m - a parameter space. Here SN_1L , SN_2R , H , BT and GH denote, respectively, the left and right saddle-node bifurcation curves (red), Hopf bifurcation curve (black), the Bogdanov-Takens bifurcation point and generalized Hopf bifurcation point.

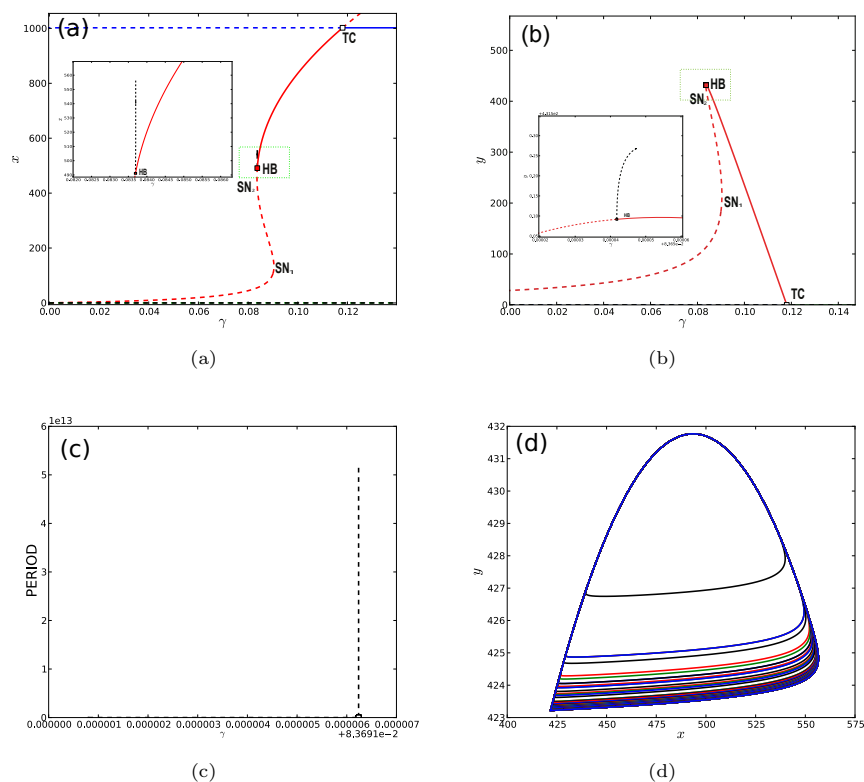


Figure 6. Bifurcation diagrams of model (2.1). HB , TC and SN_i ($i = 1, 2$) denote the Hopf bifurcation point, transcritical bifurcation and saddle-node bifurcation point. (a) One-parameter bifurcation diagram for m vs x . (b) One-parameter bifurcation diagram for m vs y . (c) Bifurcation diagram of m vs the period. (d) A family of unstable limit cycles approach a homoclinic orbit in phase portrait, and relaxation oscillations occur.

eter and keep the other parameters fixed as in (4.1) and $s = 6 \times 10^{-5}$. There is a subcritical Hopf bifurcation $HB(491.135, 432.097)$ for $m = 0.42066$, shown in Fig. 4 (a) and (b); and saddle-node bifurcation points $LP_1(190.622, 287.811)$ and $LP_2(445.949, 427.949)$ for $m = 0.557996$ and $m = 0.399977$, respectively; and one transcritical bifurcation point $TC(1002.22, 0)$ for $m = 0.95$. If the intraspecific competition is weak ($s = 10^{-5}$), the number of prey and predators will increase until m reaches the hydra effect intervals $m \in [0.399977, 0.557996]$ or $[0.399977, 0.42066]$. The corresponding multiple hydra effects region is $[0.399977, 0.42066]$. If the prey refuge becomes larger and larger, the density of prey will increase until it reaches the carrying capacity. In the meanwhile, the density of predator will decrease sharply until extinction. If we continue from the subcritical Hopf bifurcation point HB , a family of unstable limit cycles approach a homoclinic cycle. Relaxation oscillations occur, as shown in Fig. 4 (c) and (d).

To find the relation between the intraspecific competition of predators and the carrying capacity, we take s and k as the primary bifurcation parameters. There are one codimension 2 Bogdanov-Takens bifurcation point $BT(1.12523 \times 10^4, 9.42576 \times 10^3)$ at $s = 3.16394 \times 10^{-6}$, $k = 2.25887 \times 10^4$, and one Bautin bifurcation (generalized Hopf bifurcation) point $GH(61.8208, 73.2086)$ at $s = 6.17169 \times 10^{-5}$, $k = 140.389$, shown in Fig. 5 (a), where the red curve and the black curve denote the saddle-node bifurcation and Hopf bifurcation. Note that, the hydra effect region (red) is bounded by the left saddle-node bifurcation curve SN_1L and the right saddle-node bifurcation curve SN_2R . If k and s are chosen from the red region, then the predators will experience multiple hydra effects. Meanwhile, the Hopf bifurcation curve with m vs a is also given in Fig. 5 (b), where H and GH denote the Hopf bifurcation curve and Bautin bifurcation point, respectively. It indicates that there always exists one subcritical Hopf bifurcation point and one supercritical Hopf bifurcation point if a varies, with $GH(457.3381, 429.5388)$ happening at $m^* = 0.86471$ and $a = 0.0874897$, where a stable limit cycle and an unstable limit cycle coexist when $0 < m < m^*$.

Finally, we take the predator's mortality rate γ as the primary bifurcation parameter, choose $s = 7.5 \times 10^{-5}$ and keep the other parameters fixed as (4.1). Then we obtain one parameter bifurcation curve, shown as in Fig. 6 (a), (b), there are one subcritical Hopf bifurcation point $HB(491.1, 431.592)$ as $\gamma = 0.0836918$, two saddle-node bifurcation points $SN_1(132.516, 215.762)$ and $SN_2(457.048, 429.474)$ when $\gamma = 0.0904114$ and $\gamma = 0.0835675$, respectively. The multiple hydra effects occur when the mean density of predator increases in response to a greater mortality. There are two hydra effect intervals $[0.0835675, 0.0836918]$ and $[0.0835675, 0.0904114]$, while the interval $[0.0835675, 0.0836918]$ is for the occurrence of multiple hydra effects. If $r \geq 0.0836918$, there is a trophic cascade. The predator population will collapse and the system tends to the bound equilibrium $E_k(k, 0)$, where k denotes the carrying capacity of the prey. A family of limit cycles originating from the HB point approach a homoclinic cycle, shown as Fig. 6 (c), (d). Further, two-parameter (r vs a) bifurcation curves about saddle-node bifurcation and Hopf bifurcation are also given in Fig. 7. Here GH denotes the Bautin bifurcation point $GH(491.899, 431.595)$ at $\gamma = 0.0991082$, $s = 3.92942 \times 10^{-5}$. The blue region indicates the region for the occurrence of multiple hydra effects, where SN_1L and SN_2R denote the left and right saddle-node bifurcation curves, respectively. The predators will experience multiple hydra effects if s and γ are chosen from the blue region.

Note that, we find that the occurrence of relaxation oscillation in Rosenzweig-

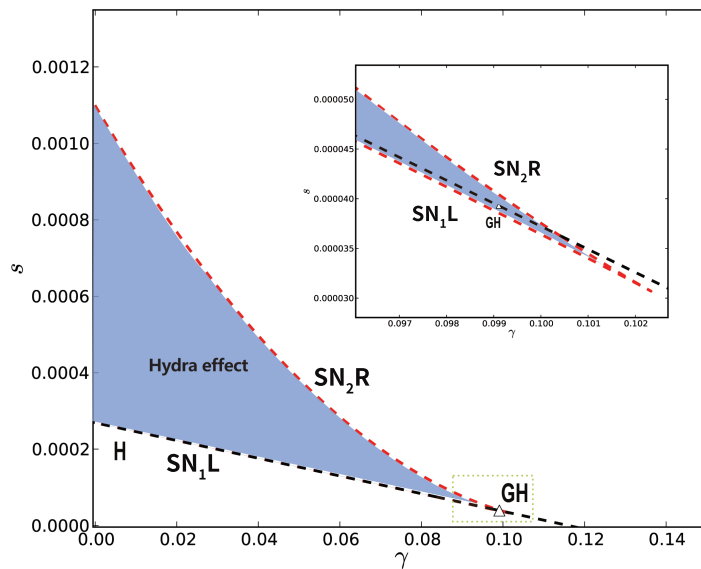


Figure 7. Two-parameter bifurcation diagram with s and γ , where SN_1L , SN_2R , H and GH denote the left and right saddle-node bifurcation curves, the saddle-node bifurcation, the Hopf bifurcation curve and Bautin bifurcation point, respectively.

MacArthur model which was mentioned in [2], this kind of very slow dynamics always denotes the fast-collapse of system. As shown in Fig 1 (d), Fig 4 (d) and Fig 6 (d), we find that the relaxation oscillation could coexist with the occurrence of the hydra effect.

5. Conclusion and discussion

To investigate the role of the predator's intraspecific competition on the relationship between predators and prey, we proposed a Rosenzweig-MacArthur model with Holling type II functional response and intraspecific competition. The model has two boundary equilibria and up to three positive equilibria. Their local and global stability were rigorously analyzed.

Moreover, we have presented a detailed analysis to prove the existence of Hopf bifurcation and conditions for stable and unstable limit cycles. The analysis consists of one-parameter and two-parameter bifurcation diagrams of the proposed system. Furthermore, the Lyapunov coefficient is used to determine the Bautin bifurcation.

Numerical simulations provide the following insights:

- (1) Once the intraspecific competition is involved, model (2.1) may have one, two, or three positive equilibria, while the original model (1.1) may only have one positive equilibrium;
- (2) Through the continuation of the half-saturation constant a , we have a supercritical Hopf bifurcation and a subcritical Hopf bifurcation in model (2.1) including the coexistence of stable and unstable limit cycles. As a comparison, there are only two supercritical Hopf bifurcation points in model (1.1);

- (3) The prey population may not decrease when the predator population increases. Nonetheless, it is important to note that there exists a parameter interval where a trophic cascade (the density of predator decreases while the density of prey increases) takes place in a one-parameter bifurcation diagram. Finally, as expected for values of γ above a critical level (where $\gamma \geq \gamma_0$, where γ_0 denotes the second saddle-node bifurcation value), the predator population collapses and the system tends to the boundary equilibrium $E_k(k, 0)$ where the prey population stabilizes at its carrying capacity. Interestingly, the hydra effect region also denotes the region with three positive equilibria, and the transition from instability to stability via Hopf bifurcation point occurs.

Note that, although Allee effect may induce the bistability and multiple hydra effects to occur, in this paper we show that the bistability is not a necessary condition for multiple hydra effects. Besides the predator's mortality rate, the intraspecific competition and prey refuge may also cause the hydra effect. More precisely, the intraspecific competition among predators has no obvious effect on the increase of the prey population but causes the predator population to increase in a range of the parameter and decrease afterward rapidly. It is interesting to observe that there are hydra effect regions for intraspecific competition, prey refuge, and the predator's mortality rate. Although the hydra effect is defined as a positive response of a population to an increased mortality rate, other parameters may produce a similar hydra effect. Biologically speaking, an increase in the mortality rate of a species, such as predation, disease, harsh environment or other factors, always intuitively leads to a decrease in its population size. However, The counterintuitive phenomenon of hydra effect indeed exists in natural populations. The further empirical and theoretical studies of hydra effect is appealing in biology since, for instance, harvesting or removal of a species is an alternative form of mortality. In this paper, we additionally find the coexistence of hydra effect and relaxation oscillations. It is intriguing to further investigate the relation between relaxation oscillations and the species' extinction, including the canard trajectories in a Rosenzweig-MacArthur model.

Acknowledgement

The authors are very grateful to Professor Guihong Fan for her helpful suggestions.

References

- [1] P. D. Adhikary, S. Mukherjee and B. Ghosh, *Bifurcations and hydra effects in Bazykin's predator-prey model*, Theor. Populat. Biol., 2021, 140, 44–53.
- [2] V. Anna, W. Sebastian and F. Ulrike, *When very slow is too fast-collapse of a predator-prey system?*, J. Theor. Biol., 2019, 479, 64–72.
- [3] L. K. Boast, E. V. Chelysheva and V. V. D. Merwe, *Cheetah translocation and reintroduction programs: Past, present, and future*, Cheetahs: Biology and Conservation, 2018, 275–289.
- [4] D. I. Bolnick, *Intraspecific competition favours niche width expansion in *Drosophila melanogaster**, Nature, 2012, 410(6827), 463–466.

- [5] L. Chen, F. Chen and L. Chen, *Qualitative analysis of a predator-prey model with Holling type II functional response incorporating a constant prey refuge*, *Nonlinear Anal.*, 2010, 11, 246–252.
- [6] P. Driessche and J. Watmough, *Reproduction numbers and sub-threshold endemic equilibria for compartmental models of disease transmission*, *Math. Biosci.*, 2002, 180, 29–48.
- [7] L. Eigentler, *Intraspecific competition in models for vegetation patterns: Decrease in resilience to aridity and facilitation of species coexistence*, *Ecol. Complex.*, 2020, 42, 100835.
- [8] S. Funk, S. Bansal, C. T. Bauch, K. T. D. Eames, W. J. Edmunds, A. P. Galvani and P. Klepac, *Nine challenges in incorporating the dynamics of behaviour in infectious diseases models*, *Epidemics*, 2015, 10, 21–25.
- [9] J. Guckenheimer and P. J. Holmes, *Nonlinear Oscillations, Dynamical Systems, and Bifurcations of Vector Fields*, Springer, 1983.
- [10] M. Haque, M. S. Rahman, E. Venturino and B. L. Li, *Effect of a functional response-dependent prey refuge in a predator-prey model*, *Ecol. Complex.*, 2014, 20, 248–256.
- [11] S. B. Hsu and J. P. Shi, *Relaxation oscillation profile of limit cycle in predator-prey system*, *Discrete & Contin. Dyn. Syst. Ser. B*, 2009, 11(4), 893–911.
- [12] Y. Huang, F. Chen and L. Zhong, *Stability analysis of a prey-predator model with Holling type III response function incorporating a prey refuge*, *Appl. Math. Comput.*, 2016, 182, 672–683.
- [13] T. K. Kar, *Stability analysis of a prey-predator model incorporating a prey refuge*, *Commun. Nonlinear Sci. Numer. Simul.*, 2005, 10, 681–691.
- [14] P. Lenka, *Regime shifts caused by adaptive dynamics in prey-predator models and their relationship with intraspecific competition*, *Ecol. Complex.*, 2018, 36, 48–56.
- [15] H. L. Li, L. Zhang, C. Hu, Y. L. Jiang and Z. D. Teng, *Dynamical analysis of a fractional-order predator-prey model incorporating a prey refuge*, *J. Appl. Math. Comput.*, 2016, 54, 435–449.
- [16] H. M. Manarul and S. Sahabuddin, *Dynamics of a harvested prey-predator model with prey refuge dependent on both species*, *Inter. J. Bifur. & Chaos*, 2018, 28(12), 1830040.
- [17] H. C. Michael and Y. Masato, *How (co)evolution alters predator responses to increased mortality: Extinction thresholds and hydra effects*, *Ecology*, 2019, 100, e02789.
- [18] H. C. Michael and A. Peter, *Hydra effects in stable communities and their implications for system dynamics*, *Ecology*, 2016, 97(5), 1135–1145.
- [19] I. S. C. Michel and A. Lucas, *Multiple hydra effect in a predator-prey model with Allee effect and mutual interference in the predator*, *Ecol. Model.*, 2018, 373, 22–24.
- [20] D. Mukherjee, *Role of fear in predator-prey system with intraspecific competition*, *Math. Comput. Simulat.*, 2020, 177, 263–275.

- [21] C. E. Parent, D. Agashe and D. I. Bolnick, *Intraspecific competition reduces niche width in experimental populations*, Ecology and Evolution, 2015, 4(20), 1–13.
- [22] J. P. Park, Y. Do and B. Jang, *Multistability in the cyclic competition system*, Chaos, 2018, 28, 113110.
- [23] S. Samanta, R. Dhar, I. M. Elmojtaba and J. Chattopadhyay, *The role of additional food in a predator-prey model with a prey refuge*, J. Biol. Syst., 2016, 24, 345–365.
- [24] S. Sarwardi, S. Ray and P. K. Mandal, *Analysis of a competitive prey-predator system with a prey refuge*, Biosystems, 2012, 110(3), 133–148.
- [25] G. Seo and D. L. DeAngelis, *A predator-prey model with a Holling type I functional response including a predator mutual interference*, J. Nonlinear Sci., 2011, 21, 811–833.
- [26] M. Sieber and F. M. Hilker, *The hydra effect in predator-prey models*, J. Math. Biol., 2011, 64, 341–360.
- [27] C. S. B. D. Silva, K. R. Park and R. A. Blood, *Intraspecific competition affects the pupation behavior of spotted-wing drosophila*, Scientific Reports, 2019, 9(1), 7775.
- [28] A. Singh, H. Wang, W. Morrison and H. Weiss, *Modeling fish biomass structure at near pristine coral reefs and degradation by fishing*, J. Biol. Syst., 2012, 20, 21–36.
- [29] J. P. Tripathi, S. Abbas and M. Thakur, *Dynamical analysis of a prey-predator model with Beddington-DeAngelis type function response incorporating a prey refuge*, Nonlinear Dyn., 2015, 80, 177–196.
- [30] H. Wang, W. Morrison, A. Singh and H. Weiss, *Modeling inverted biomass pyramids and refuges in ecosystems*, Ecol. Model., 2009, 220, 1376–1382.
- [31] H. Wang and S. Thanarajah, *Refuge-mediated predator-prey dynamics and biomass pyramids*, Math. Biosci., 2018, 298, 29–45.
- [32] H. S. Zhang, Y. L. Cai, M. S. Fu and W. M. Wang, *Impact of the fear effect in a prey-predator model incorporating a prey refuge*, Appl. Math. Comput., 2019, 356, 328–337.